AIR-SEA COUPLING OF INDIAN OCEAN AND ITS CLIMATIC RESPONSES

Final Synopsis

Submitted for the award of the Degree of Doctor of Philosophy

Submitted to

Department of Physics
Mangalore University
Mangalagangotri - 574199

Submitted by

Nisha P. G.
Reg No.-178105117

Under the guidance of

Prof. T. S. Pranesha

Department of Physics
BMS College of Engineering
Bengaluru- 560019

May 2024

Name of the Candidate	**: Nisha PG**
Title of Thesis	**Air-Sea Coupling of Indian Ocean and its Climatic Responses**
Name of the Research Supervisor	**: Prof. TS Pranesha**
Name of the Institution	**: Department of Physics, BMS College of Engineering**
Date of Registration	**: 29th June 2018** **University letter No.** **MU/EXB/Ph.D./CR.19/Phy./2020-21/E.13** **Dated: 01.06.2020**
Date of Colloquium	**: 20.03.2024**

1. Introduction

This thesis focuses on examining variations in Indian ocean heat content and its relationship with atmospheric parameters, particularly wind, convection, and the LLJ. Investigating the large-scale spatial and temporal variability of air-sea fluxes provides insights into both thermodynamic (heat content) and dynamic (wind) forcing mechanisms in the Indian Ocean. The interaction between surface processes and synoptic weather patterns in the Indian Ocean remains inadequately understood, motivating a systematic investigation in this study for both weather forecasting and climate research purposes. The research delves into the decadal dynamics of the Indian Ocean and its impact on atmospheric winds. Furthermore, efforts are made to comprehend recent trends in Indian Ocean warming and heat content, and their influence on convection and wind circulation. The systematic study of the above-mentioned parameters with respect to the Indian Ocean can help in better understanding the extremes in the climatic conditions and the monsoon and that in turn has a major impact on the Indian trade and economy.

2. Review of Literature

The Indian Ocean, with its closed northern boundary and its link to the Pacific and Southern Oceans, has warmed rapidly and monotonically (Lee et al., 2015; Levitus et al., 2009; Yang et al., 2020). Global and regional changes in heat content are strong indicators of climate change and understanding climate change, both past and future, is crucial. The extremes caused by global warming have a much greater impact on the environment and society. For example, heatwaves, drought, wildfires, frequent heavy rainfall episodes and risks of flooding are associated with increased water vapour and higher temperatures in the environment (Lin and Shullman, 2017). It is important to understand the long-term variability of heat content to explore the modulation of such variability by anthropogenic trends. The warming trend has been observed over the global ocean (Levitus et al., 2012), but the Indian Ocean has demonstrated relatively strong warming (Dong et al., 2014; Du and Xie, 2008; Han et al., 2014b; Lee et al., 2015; Nieves et al., 2015) along with associated sea-level rise (Deepa et al., 2018; Han et al., 2014b; Lee and McPhaden, 2008; Nidheesh et al., 2013; Srinivasu et al., 2017; Swapna et al., 2017; Thompson et al., 2016). It

appears that this small basin is playing an outsized role in modulating the global ocean response to anthropogenic emission increases.

The impact of warmer temperature anomalies across the Indian Ocean over shorter timescales on regional and global climate (Annamalai and Murtugudde, 2004; Han et al., 2014b, 2014a; Schott et al., 2009) such as the strengthening of the Pacific Walker circulation (Luo et al., 2012), the El Niño-Southern Oscillation (ENSO) variability (Yu, 2008; Yu et al., 2002) and its relationship with Indian monsoon (Gadgil et al., 2007; Murtugudde et al., 2000; Saji et al., 1999; Ummenhofer et al., 2011; Webster et al., 1999) have been identified. Decadal variations in Indian Ocean Sea Surface Temperature (SST) were also associated with the tropical storm intensity of that region (Evan et al., 2011; Krishna, 2009; Rao et al., 2008; Wang et al., 2012) and increasing heat content (Vidya et al., 2021). As the thermal energy not only from the Mixed Layer (ML) but also from the layers below is required for the development of cyclones and most marine weather events. Tropical cyclone heat potential and heat content has been utilized in numerous studies (Ali et al., 2018; Murty et al., 2006; Nagamani et al., 2016) rather than SST as a suitable parameter to study. Elevated heat content tends to prolong the lifetime, intensity and increase the occurrence of storms, thereby leading to increased rainfall (Balaguru et al., 2014; Trenberth et al., 2018). Roxy et al. (2017) noted that it receives most of the moisture input during widespread monsoon extremes due to Arabian Sea warming.

Indian Ocean Dipole (IOD) has been studied for its impact on Indian summer monsoon rainfall. During its positive phase, IOD exhibits cold SST anomalies near Sumatra and warm SST anomalies in the western Indian Ocean. This pattern was accompanied by corresponding wind and precipitation anomalies (Gadgil et al., 2007; Murtugudde et al., 2000; Saji et al., 1999; Webster et al., 1999) as well as wind-driven effects over the ocean (Gadgil et al., 2004; Saji and Yamagata, 2003; Yamagata et al., 2004). The southwest monsoon winds across the Arabian Sea and the Bay of Bengal are stronger during positive IOD events (Vinayachandran et al., 2002). Sayantani et al. (2014) suggested that the evolution of IODs is significantly influenced by the spring warming of the Arabian Sea and the associated summer barrier layer. Their research indicates that easterly wind anomalies are caused by convection and warmth in the west, long before there is any noticeable eastern cooling in IOD years. It has been observed that IOD occurs both with and

without ENSO (Wang et al., 2016; Yamagata et al., 2004) and the debate about whether IOD is independent of ENSO continues (Wang et al., 2016). The asymmetry in the ENSO teleconnection to this region is observed to be a determinant of the summer long-term warming across the western Indian Ocean. (Roxy et al., 2014). The increasing temperatures are also blamed for the coral bleaching that is threatening the biodiversity in the Indian Ocean (Zinke et al., 2015). In this context, it is evident that the low-frequency heat content variability over the North Indian Ocean (NIO) is critical for this region which is highly vulnerable to climate variability and change.

A rapid increase in the Indian Ocean heat content down to 700 m, which accounts for more than 70% of the global ocean heat content was observed during 2003-2012 (Lee et al., 2015). The heat content variations in the upper 700 m of the Pacific and Indian Oceans are linked to the hiatus of the global mean surface warming (Liu et al., 2016). Previous studies have reported a decrease in heat content in the upper layers of the Pacific Ocean (Balmaseda et al., 2013; Meehl et al., 2011) with an increase in the Indonesian Throughflow (ITF) heat transport. According to Nieves et al. (2015), warming in the Indian Ocean's subsurface (100–300 m) counterbalance the cooling in the top 100 m of the Pacific Ocean.

The warming in the Southern Tropical Indian Ocean (STIO) was attributed to the horizontal advection from the ITF region increasing the upper ocean heat content over the STIO (Murtugudde and Busalacchi 1999; Zhang et al. 2018; Vidya et al. 2020). The study also revealed the major role of the phases of Pacific Decadal Oscillation (PDO) in the subsurface cooling in SIO. Impacts of the ITF on regional and global climate have been reported (Murtugudde et al., 1999; Sprintall et al., 2014). The global hydrological cycle is affected by surface evaporation caused by wind. Other than the thermal expansion, wind-driven circulation changes affect the regional sea level variations. Timmermann et al. (2010) showed that the changes in the prevailing wind regimes are largely responsible for the decadal and multidecadal sea level trends in the tropical Indo-Pacific region. The zonal wind change exhibits high uncertainty in the equatorial Indian Ocean (Han et al., 2014b). Previous studies using ocean models suggested that the wind forcing over the Indian Ocean, influenced by remote forcing from the Pacific through the ITF, is a primary factor that modulates the basin-wide decadal sea level variation patterns (Trenary and Han, 2008). Indian Ocean heat content shows maximum variability in the upper 700 m. This is because the upper layers of the ocean have the most interaction with atmospheric wind, radiation, and turbulent heat fluxes, which exhibit significant diurnal and seasonal variations (Ali et al., 2018). It has been

proposed that the main cause of the rise in oceanic heat is the strengthening of the shallow overturning cells in the Pacific Ocean caused by the trade wind (Balmaseda et al., 2013). The strength of the winds impacts the surface turbulent heat flux and the cross-equatorial heat transport in the NIO, thus maintaining the NIO heat balance (Srinivasu et al., 2017).

Convection is a crucial factor that regulates the hydrological cycle over Earth. Over the tropics, the intraseasonal variations of deep convection is well-organized large-scale disturbances, with its peak amplitude over the Indo-Pacific region, with its strong seasonality over the Indian Ocean (Duvel and Vialard, 2007). During summer, this convective disturbance transmits from the equator northward to the Indian peninsula and its peak amplitude is found to be over the Bay of Bengal. In contrast to this, in winter its peak amplitude is located between the equator and 15°S propagating eastward from the western Indian Ocean to the central Pacific generally known as Madden–Julian oscillation (MJO) (Madden and Julian 1994). Sengupta and Ravichandran (2001) showed SST perturbations of up to 3 K in relation to the intraseasonal variability of the convection in the Bay of Bengal.

The low-level jet over the Indian Ocean has correlations with the oceanic parameters and acts as a major force for the monsoon winds. Associated with the Hadley circulation, the Low-Level Jetstream (LLJ) is a primary feature of the Asian summer monsoon (Krishnamurti et al., 1976). Originating from the easterly trade winds of the south Indian Ocean, LLJ is a cross-equatorial phenomenon (Findlater, 1969). LLJ turns westerly over the Arabian Sea and passes through peninsular India and the Bay of Bengal. Deepa et al. (2007) showed the formation of an onset vortex in the shear line of the northern part of LLJ over the Mini Warm Pool in the East Arabian Sea. Another study by (Praveen et al., 2020) showed the poleward shift of LLJ maintains the MLD intact in the northern Arabian Sea. Hence, it is very important to study the variations of LLJ with respect to heat content, as the ocean and atmosphere near to ocean are always interconnected.
This research work involves the study of variations in the heat content of the Indian Ocean and its relation with the atmospheric parameters, mainly wind, convection and the LLJ. The study of large-scale spatial and temporal variability of air-sea fluxes gives an insight into the thermodynamic (heat content) and dynamic (winds) forcing over the Indian Ocean. The interplay between the surface processes and the synoptic weather pattern over the Indian Ocean is not well

understood and this study systematically investigates this interplay for both weather forecasting and climate research purposes. In the present study, the decadal variation of Indian Ocean dynamics and its effect on atmospheric winds has been analyzed. Attempts are also made to understand the recent trends of the Indian Ocean warming and heat content, and its effect on convection and wind circulation.

3. Objectives of the proposed research

The systematic study of the above-mentioned parameters with respect to the Indian Ocean can help in better understanding the extremes in the climatic conditions and the monsoon and that in turn has a major impact on the Indian weather, trade and economy. The major objectives of the thesis are given below.

- To study the inter-annual and decadal variations of heat content over the Indian Ocean and its causative mechanism.

- To establish the relation between heat content, wind and convection over the Indian Ocean on different time scales.

- To study the possible relation between the oceanic heat content and Low-Level Jet (LLJ).

4. Methodology followed

Data:

Various atmospheric and ocean parameters used in the present study use *in situ*, satellite and reanalyses data. This study uses Low-Resolution Monthly Time Series (LRMTS) lightning data with a spatial resolution of 2.5°×2.5° from January 1996 to December 2013. The data of LFR are retrieved from https://ghrc.nsstc.nasa.gov/lightning/data/data_lis_otd-climatology.html.

The study requires monthly data for turbulent heat fluxes, such as Latent Heat Flux (LHF), Sensible Heat Flux (SHF), humidity, zonal and meridional components of wind velocity, Outgoing Longwave Radiation (OLR) and Convective Available Potential Energy (CAPE). These data are taken from ECMWF Re-Analysis 5 (ERA5), which is accessible at https://www.ecmwf.int/en/forecasts/datasets/reanalysis-datasets/era5, with a resolution of 0.25°×0.25°. 10 m zonal winds are taken from ECMWF ERA-Interim analysis (Dee and

Coauthors, 2011) and are obtained from https://www.ecmwf.int/en/forecasts/datasets/reanalysis-datasets/era-interim.

The monthly ocean potential temperature and salinity data are obtained from ECMWF Ocean Reanalysis System 4 (ORAS4) at a resolution of 1°×1° with 42 levels in the vertical for computing heat content (Balmaseda et al., 2013). The data from 1958 to 2017 is available at http://www.ecmwf.int/products/forecasts/d/charts/oras4/reanalysis/.

The updated version of monthly mean ocean potential temperature and zonal and meridional currents in the ocean at a spatial resolution of 0.25°×0.25° in the horizontal with a near-surface vertical resolution of 1 m is obtained from ECMWF Ocean Reanalysis System 5 (ORAS5) (Balmaseda et al., 2013). The data from 1979 to present is retrieved from http://www.ecmwf.int/products/forecasts/d/charts/oras4/reanalysis/.

DMI defines the intensity of the IOD and is computed by the gradient of SST between the western (from 50°E to 70°E and 10°S to 10°N) and the southeastern equatorial Indian Ocean (from 90°E to 110°E and 10°S to 0°N) (Saji et al. 1999). HadISST1.1 is used to estimate DMI, which may be accessed at https://psl.noaa.gov/gcos_wgsp/Timeseries/Data/dmi.had.long.data. In the present study, September-October-November mean DMI is used.

ONI is computed from ERSST.v5 SST anomalies (3-month running mean) of in the east-central tropical Pacific Niño 3.4 region over 5°N to 5°S and 120° to 170°W (Source: https://origin.cpc.ncep.noaa.gov/products/analysis_monitoring/ensostuff/ONI_v5.php). We have employed ONI for the months of October-November-December in this study. PDO index used in the present study is the standardized value derived as the leading principal component of monthly SST anomalies in the North Pacific (north of 20°N) following Mantua et al. (1997). The data is obtained from JISAO PDO Index from http://jisao.washington.edu/pdo/PDO.latest.txt

The ORAS4 temperature and salinity are compared with in-situ Argo data (http://apdrc.soest.hawaii.edu/las/v6) and surface zonal and meridional currents are compared with Surface Current Analyses Real-time (OSCAR) data (https://podaac.jpl.nasa.gov/dataset/OSCAR_L4_OC_third-deg) to check the suitability of the data for the study in the Arabian Sea region.

Calculation of Heat Content:

The heat content is calculated following Vidya et al., 2020, using the equation:

$$OHC = \rho_0 C_p \int_{h_1}^{h_2} T(z)dz \qquad (1)$$

where ρ_0 is the reference seawater density (1027 kg m^{-3}), C_p is the specific heat capacity of seawater at constant pressure, p; h_1 and h_2 are the depths of integration between which heat content is calculated, and T is the ocean potential temperature.

Moisture advection:

Moisture advection is computed using the below equation:

$$\frac{dq}{dt} = -[u\frac{dq}{dx} + v\frac{dq}{dy} + z\frac{dq}{dz}] \qquad (2)$$

where, q is specific humidity, u, v, and w are zonal, meridional and vertical components of wind velocity, respectively. In this study, only the horizontal moisture advection is considered using zonal and meridional components of wind.

Zonal and meridional components of volume and heat transport

Zonal and meridional components of volume and heat transport are calculated using zonal and meridional components of ocean currents as given below.

Meridional Volume Transport = $\iint \vec{v}\, dA$ (3)

Meridional Heat Transport = $\iint \rho_{water} C_p T\, \vec{v}\, dA$ (4)

where $\vec{v}$ is the meridional ocean currents, ρ_{water} is the density of sea water calculated from temperature and salinity, T is the seawater temperature, and A is the area of integration.

Cross equatorial winds are calculated from the time merged data of meridional component of wind data from ERA-40 data for 1960-1979 and ERA-Interim from 1980-2017 at 850 hPa, averaged over 5°S to 5°N and 37.5°E to 60°E.

Cross equatorial volume and heat transport are obtained by integrating the meridional volume and heat transport over 37.5°E to 60°E and 5°S to 5°N.

LLJ is calculated by the average of zonal wind anomaly over 8°N to 14°N and 50°E to 70°E.

Mascarene High is computed from the average of sea level pressure anomaly over 35°S to 20°S and 40°E to 90°E.

Multiple regression model

For the comprehensive analysis of the dependence of LFR on heat content and moisture advection from the Arabian Sea and Bay of Bengal, a multiple regression model is used. By explaining the

relationship between a dependent variable and many independent variables, this statistical technique is used to model and analyse multiple variables.

Y is a length-i one-dimensional array that holds the dependent variable yi. X is a two-dimensional array of size (i,n), with n representing the number of independent variables.

$$y_i = b_0 + b_1 x_{i1} + b_2 x_{i2} + b_3 x_{i3} + \cdots + b_n x_{in} \quad (5)$$

Eq (5) represents the least square regression line for multiple regression of *n* independent variables where, b_0 is the y-intercept (constant term), x_{in} is the nth independent variable and $b_n$is the coefficient of the nth independent variable. When all the independent variables $x_{i1}, x_{i2} \ldots \ldots x_{in}$ are constant, the predicted value of y_i is b_0.

Empirical Orthogonal Function

To study the interannual variability in detail, we performed an Empirical Orthogonal Function (EOF) analysis on the seasonal mean of heat content down to 300 m, over the Arabian Sea from 2000 to 2017.

Calculation of Heat Budget

Strong winds and high surface salinity are two characteristics of the Arabian Sea that promote vertical mixing (Prasanna Kumar and Prasad, 1999). Air-sea heat fluxes, advective-diffusive processes, and entrainment at the mixed layer's base all have an impact on the heat stored in the ocean's surface mixed layers. The depth at which the temperature drops by one degree Celsius from its surface value is used to calculate the MLD in the Arabian Sea (Prasanna Kumar and Narvekar, 2005). The heat budget is then computed in the ML after Dong et al. (2007) and is given by the equation below:

$$\frac{\partial T_m}{\partial t} = \frac{Q_{net} - Q(-h_m)}{\rho_0 c_p h_m} - u_m . \nabla T_m + \kappa \nabla^2 T_m - \frac{w_e \triangle T}{h_m} \quad (6)$$

is the MLD, T_m is the ML temperature, ρ_0 is the reference density of seawater (here 1027 kg m^{-3}), C_p is the specific heat capacity of seawater at constant pressure (4000 J kg^{-1} K^{-1}), κ is the eddy diffusivity and w_e is the entrainment velocity. $Q(-h_m)$ is the downward radiative heat flux at the

bottom of the ML. The first term on the right side of eq. (2) denotes the air-sea heat flux term where $Q(-h_m)$ is calculated based on the assumption of exponential decay with depth (Qiu and Kelly, 1993) using the equation,

$$Q(-h_m) = Q(0)\left[Re^{\left(\frac{-h_m}{\gamma_1}\right)} + (1-R)e^{\left(\frac{-h_m}{\gamma_2}\right)}\right] \qquad (7)$$

where, $Q(0)$ is the shortwave radiation flux at the sea surface and R, γ_1, γ_2 are the constants 0.67, 1 and 17, respectively (Dong et al., 2007). Q_{net} is taken as positive into the ocean.

The horizontal ocean heat advection is represented by the second term in eq. (2). The term $u_m.\nabla T_m$ is used to compute zonal and meridional ocean heat advections within the MLD, from zonal and meridional components of currents, respectively, from ORAS4. Here ∇T_m denotes the temperature gradient.

The third term represents diffusion. The contribution from the diffusion term of eq. (2) the long-term interannual variability is small and hence is not considered in this study. The entrainment of water from the ML's base is described by the final term in equation (2). The entrainment term is calculated from $\frac{w_e \triangle T}{h_m}$, where $\triangle T$ is the difference in temperature between the mixed layer and the layer just below it.

4. Outcome of the proposed research

(a) Trend and Interannual Variability of the Arabian Sea heat content

The unpredictability in the monsoon variability and the extremes are significantly influenced by changes in the Arabian Sea. The Indian Ocean rim countries, which are greatly prone to climate change effects are extremely concerned about the notable warming over this region during the recent decades. The purpose of the present study was to provide some insight into the heat content variability and trend of this critical region, particularly with regard to the processes that at lower frequencies, are driven by the long-term memory of the subsurface heat content and on relatively fast timescales, feedback to the atmosphere with the ML heat content. We must identify the drivers of heat content for each season due to the seasonality of the region. The trend of monthly anomaly of heat content from the surface to a depth of 300 m over the Arabian Sea (averaged over 5°N to

25°N and 60°E to 72°E), from 1960 to 2017 shows consistent upward trend in heat content from 2000 to 2017 with greater warming over this period. In the Arabian Sea, during the spring and summer, heat content exhibits high variability, or the largest standard deviation, to the north of 8°N; in the autumn and winter, maximum variability is recorded to the south of 20°N, encompassing a greater area (Fig.2).

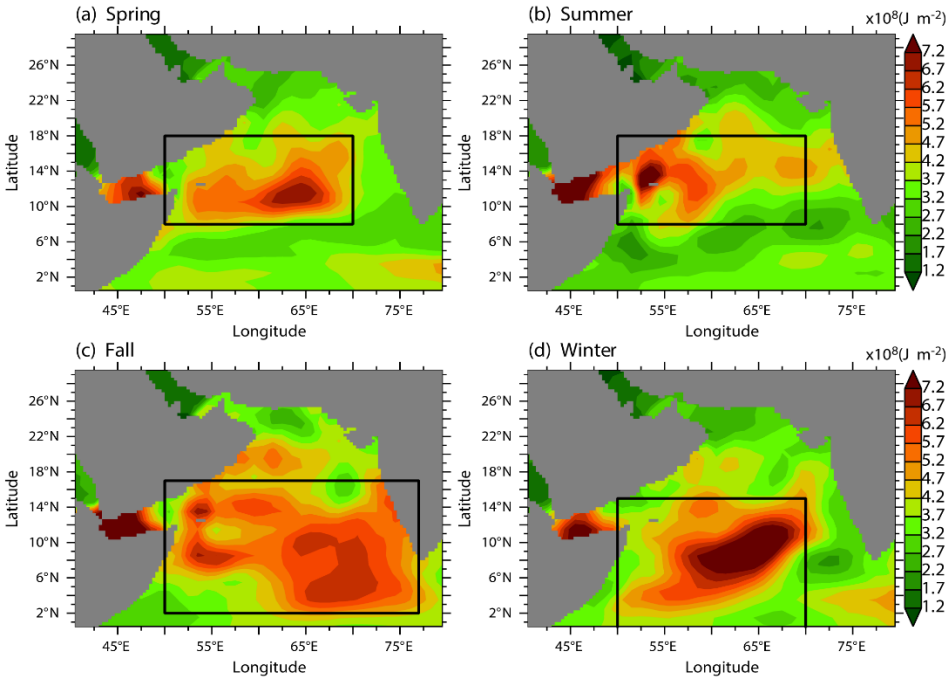

Fig. 2. Standard deviation of heat content down to 300 m for (a) spring, (b) summer, (c) fall and (d) winter seasons

Figure 3 shows the time series and long-term trends of the seasonal mean of heat content anomaly in the upper 300 m for all four seasons over the observed regions of maximum variability during the period 2000-2017. According to the results obtained, the heat content increase below the MLD is mostly responsible for the significantly growing trends in heat content in the upper 300 m during the spring and summer (Fig. 3c), whereas the heat content in ML is primarily responsible for the trends in fall and winter (Fig.3b). The rising trend in heat content seen in the Arabian Sea during the period of study is explained by an increase in ocean heat convergence driven by an increasing trend in thermocline depth. The strongest ENSO warming peak of 2015-16 was observed only in heat content below MLD, and the positive, significant correlations between heat content and ENSO demonstrate that ENSO affects the interannual variability of heat content below the ML while other factors, such as air-sea fluxes, have an impact on heat content in the ML. A noteworthy association between the heat content in and below the ML is also demonstrated by the study,

suggesting the possibility of heat exchange between the surface and subsurface layers throughout the year, with a prolonged memory in the fall and winter.

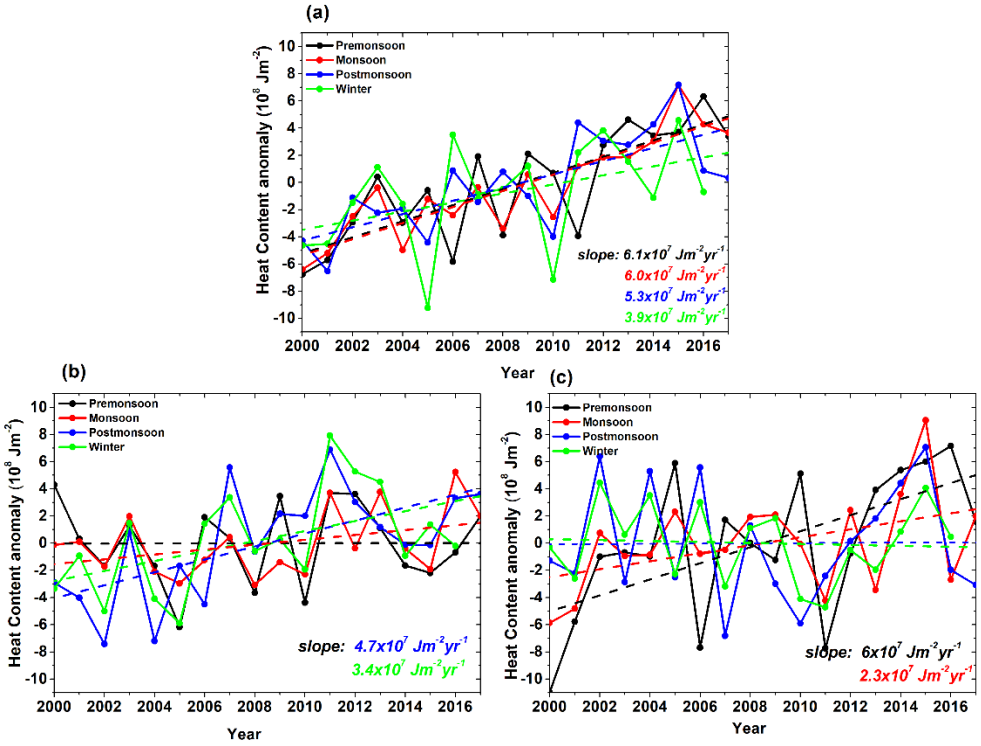

Fig. 3. Heat content anomaly (solid line) and trend (dashed line) (a) for a depth of 300 m, (b) above the MLD and (c) below the MLD down to 300 m during spring (black), summer (red), fall (blue) and winter (green) seasons. Slopes of significant trends (>90%) are listed in each box

Variations in air-sea fluxes throughout fall and winter are the primary causes of the interannual variability of ML heat content, indicating a practically one-dimensional equilibrium during these seasons. But ENSO and IOD also contribute significantly to the variability in fall and winter, respectively. With remote forcing from ENSO and IOD, thermocline changes appear to be a major factor driving the interannual variability in heat content below the MLD throughout spring.

Ekman transports into and out of the Arabian Sea are implicated as a major activity during the summer months due to the importance of thermocline variability and ocean advection. According to this study, the heat content of the Arabian Sea continues to rise with an increase in positive IOD and El Niño years along with an increase in air-sea fluxes; nevertheless, multi-decadal variability cannot yet be fully ruled out.

The results are also confirmed using Empirical Orthogonal Function (EOF) analysis (Tables 2 and 3).

Parameters	Fall		Winter	
	PC1	PC2	PC1	PC2
DMI (SON)	0.34	0.41**	0.51**	0.28
ONI(OND)	-0.61**	-0.16	-0.13	0.28
Zonal wind	0.38	-0.04	0.07	-0.31
Air-sea flux	-0.42**	-0.17	-0.77**	0.09
Zonal Ocean advection	0.32	-0.21	0.13	0.21
Meridional Ocean advection	0.71**	0.01	-0.27	-0.67**

**- above 90% significant; PC- Principle component of EOF analysis

Table. 2 Correlation coefficients of PC1 and PC2 of heat content above MLD with DMI, ONI, zonal winds, air-sea flux and ocean advection

Parameters	Spring		Summer	
	PC1	PC2	PC1	PC2
D20	0.73**	0.40**	0.55**	0.58**
DMI (SON)	*0.44***	*-0.47***	*-0.08*	*0.35*
ONI(OND)	*0.72***	*-0.42***	*0.01*	*0.07*
Zonal Ocean advection	-0.40**	-0.14	-0.13	0.15
Meridional Ocean advection	0.29	-0.03	-0.33	-0.40**

**- above 90% significant*; Italic values - the lag correlation of PC with preceding year DMI and ONI values*; PC- Principle component of EOF analysis

Table 3 Correlation coefficients of PC1 and PC2 components of heat content below MLD, with D20, DMI, ONI and ocean heat advection

Previous research demonstrated that IOD and ENSO are the primary climate modes responsible for interannual variability in the tropical Indian Ocean. Therefore, we tried to investigate in this study whether these occurrences have any impact on the Arabian Sea's long-term and interannual variability in heat content.

(b) Decadal Variability of heat content in the North Indian Ocean

In this study, we examine the decadal variability of HC in the NIO from the surface to a depth of 700 m and explore their causes. The wavelet spectra reveal an evident ~10-11-year signal in NIO HC contributed mainly by the Arabian Sea region. The analysis is done for the three periods namely, the cold phase of PDO 1960-1977 (phase I), the warm phase of PDO 1978-2002 (phase II), and the cold phase of PDO 2003-2017 (phase III). The decadal variations of the HC show moderate variability during the first cold PDO phase I and warm PDO phase II but show a rapid increase in the second cold PDO phase III (Fig. 4).

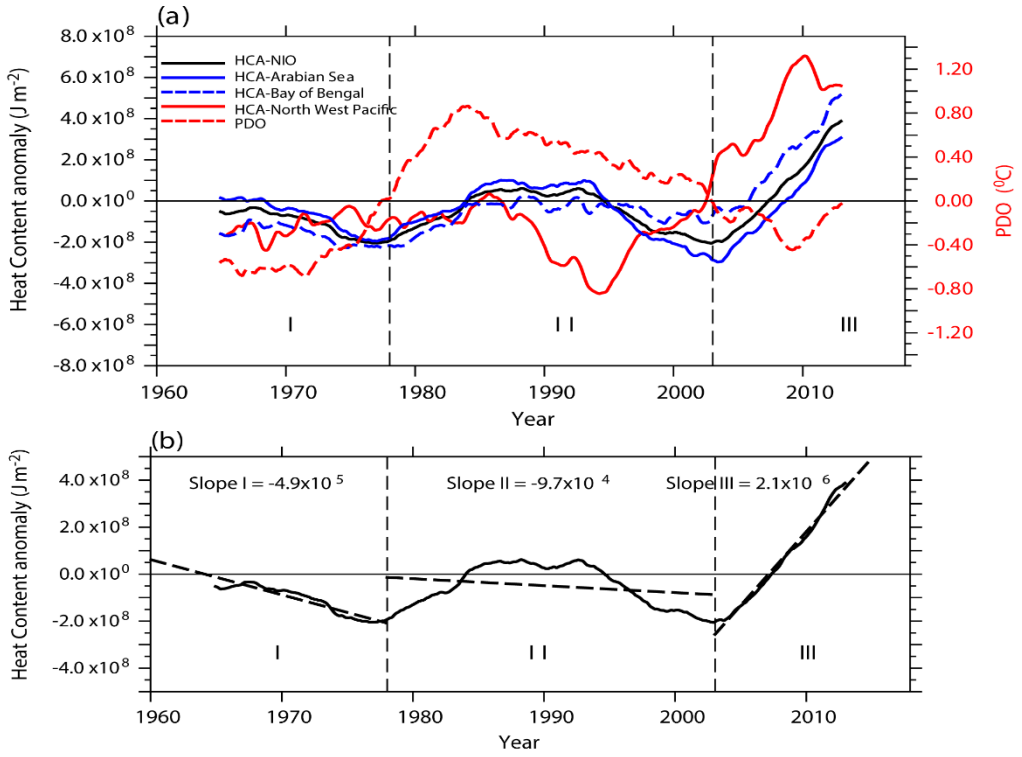

Fig. 4. 10-year running mean of HC anomaly from surface to 700 m for NIO (black line), Arabian Sea (blue line) and Bay of Bengal (blue dash), North West Pacific (red line), PDO (red dash)

Throughout the period of study, the variations in HC over the NIO show an anti-phase relation with PDO, except for the mid-1980s to mid-1990s in phase II, which shows a significant warming. A detailed analysis of the vertical structure of the temperature anomaly in NIO shows that the maximum heat stored in phase III lies within a depth of 300 m. The robust increase in HC in the NIO during phase III is observed to be consistent with the increase in HC over the Northwest

Pacific. Moreover, the large increasing trend in HC during phase III and northward increasing currents from SIO also assist this increase in heat over NIO.

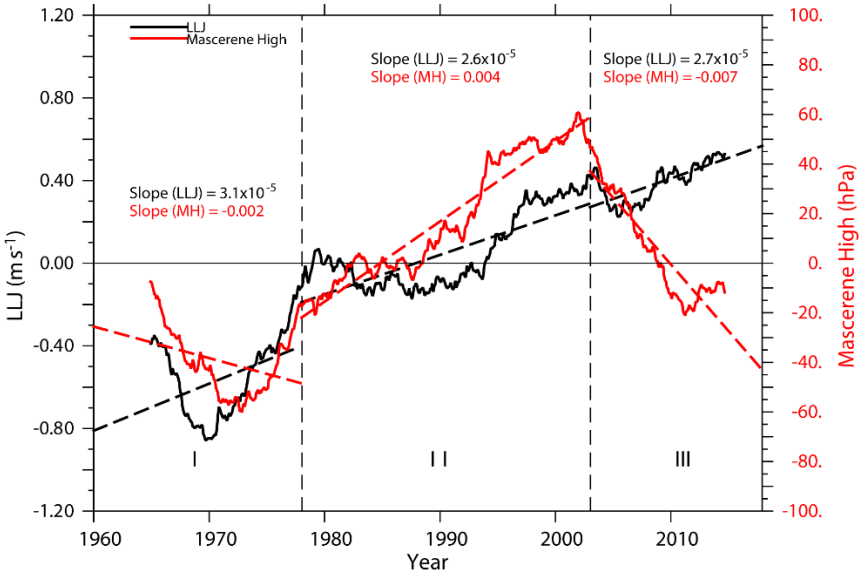

Fig.5. 10-year running mean of LLJ (black), Mascarene High (red) and their trends (dashed line). All the trends are significant above 95% confidence level.

During phase I, low values of LLJ and cross-equatorial transports drive less heat northward from the SIO (Fig. 5, black line). During phase III, LLJ shows a significant increase in strengthening, and Mascarene High shows a significant weakening trend (Fig. 5, red line). This Mascarene High weakening is owed to the increase in SST over the region triggered by the heat transport from the Pacific. The strengthening of LLJ drives a cross-equatorial meridional volume and heat transport. The cross-equatorial meridional volume and heat transports from SIO to NIO show their peak value at 300 m during phase III, hence causing a substantial increase in HC over the region.

The present study highlights the role of the Pacific in the rapid accumulation of heat in NIO and the cross-equatorial heat transfer from the SIO, on a decadal timescale. These findings will help in interpreting the increase in heat over the tropical Indian Ocean that has resulted in increasing cyclone activity in the NIO. Systematic studies in this direction would be useful for both weather forecasting and climate research purposes in this climate-vulnerable region.

(c) Differential warming over the Indian Ocean

Examining differential warming over the Indian Ocean, it explains the opposite patterns of warming across the Indian Ocean during the recent decade spanning from 2010 to 2022 (Fig. 6a), with a specific focus on the Arabian Sea and the Bay of Bengal. The analysis compares the contrasting years of 2010 and 2019, characterized by divergent heat content patterns in these two regions, for further examination.

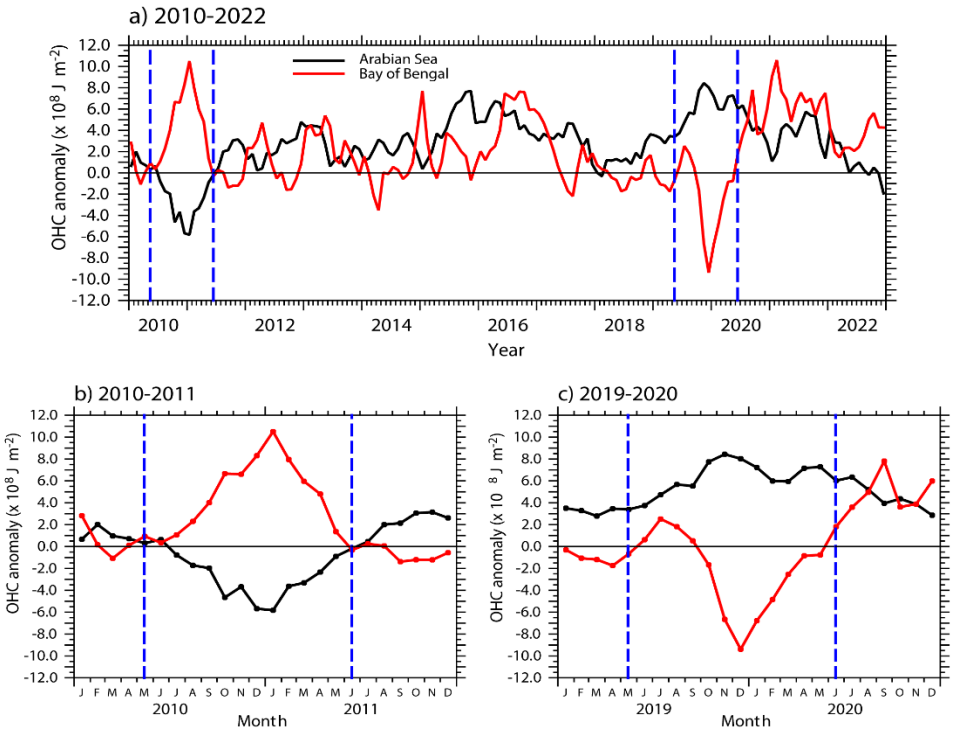

Fig. 6. Monthly mean Heat content anomaly for Arabian Sea (black line) and Bay of Bengal (red line) from (a) 2000-2022, (b) 2010-2011 and (c) 2019-2020.

During 2010, the Bay of Bengal experienced warmer conditions characterized by a deeper thermocline, heightened convection, and increased rainfall, whereas the Arabian Sea exhibited cooler temperatures alongside a shallow thermocline, reduced convection, and rainfall. Conversely, in 2019, the conditions were reversed, with the Arabian Sea displaying warmer temperatures and the Bay of Bengal experiencing cooler conditions.

The study scrutinizes the temporal lag observed in the association between the peak phase of the IOD during September-October-November and the maximum heat content during winter.

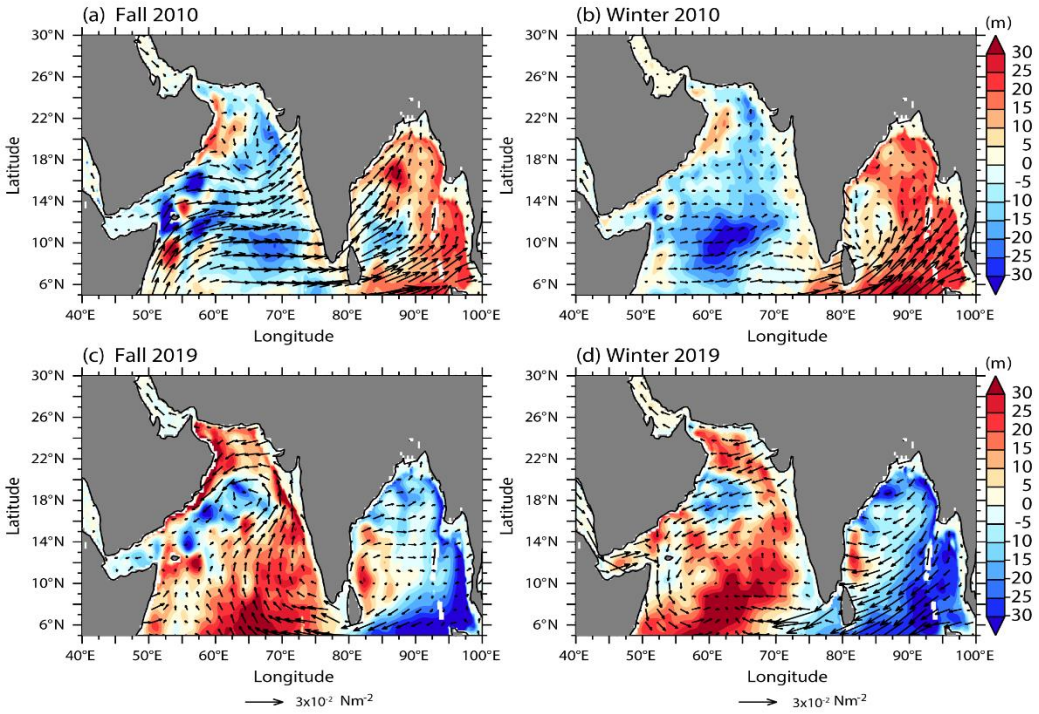

Fig. 7. Seasonal climatology of D20 anomaly (shaded) and wind stress anomaly (vectors) for (a) fall 2010, (b) winter 2010, (c) fall 2019 and (d) winter 2019.

Additionally, the study sheds light on the disparity in cyclone occurrences between the two years, with a higher frequency of cyclones (including Depressions, Cyclonic Storms, and Severe Cyclonic Storms) observed in the Arabian Sea during 2019, while in 2010, they were more prevalent in the Bay of Bengal compared to the Arabian Sea. This comprehensive analysis provides valuable insights into the dynamic interplay between oceanic and atmospheric phenomena across the Indian Ocean, elucidating the intricate relationships between temperature variations, thermocline depths, convection patterns, rainfall distribution, and cyclone occurrences in the AS and BOB during the specified period.

(d) Role of North Indian Ocean on the Lightning Flash Rate (LFR) of the Indian Land Region

Figure 1 displays the seasonal climatology calculated from monthly LFR data for the Indian area from 1996 to 2013.

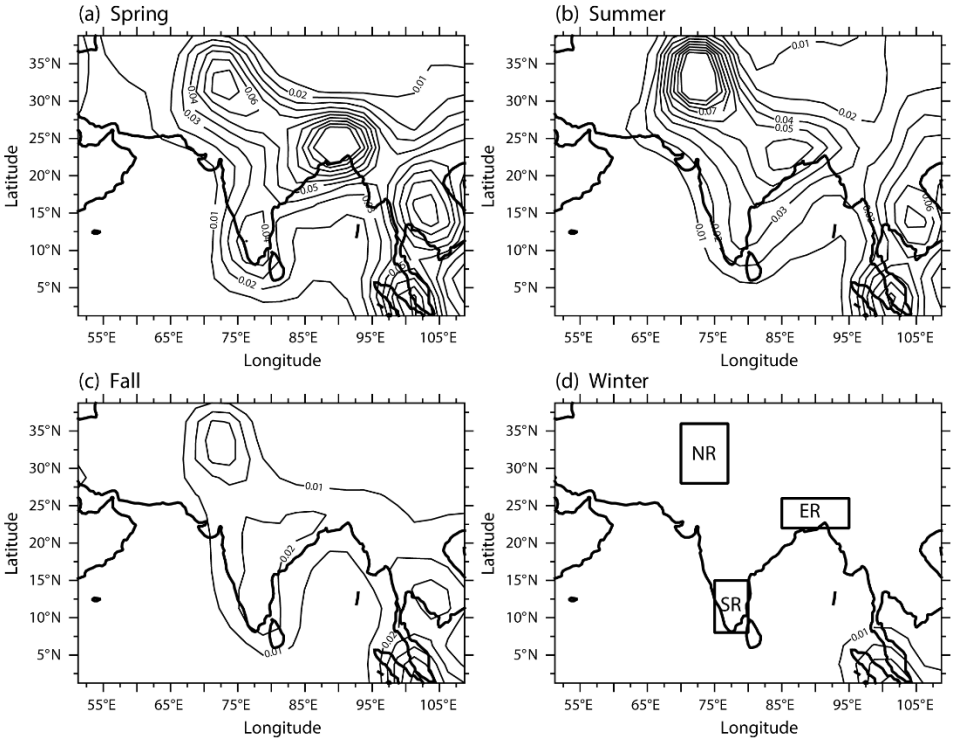

Fig. 1. Climatological spatial variations of LFR (counts km-2day-1) during four seasons, a pre-monsoon, b monsoon, c post-monsoon and d winter during 1996 to 2013.

The North, Northeast, and South Peninsula regions are the three areas where LFR is most prevalent. As illustrated in figure 1d, the areas with peak LFR for detailed analysis are identified as the North region (NR; 28°N-36°N; 70°E-77°E); East region (ER; 22°N-26°N; 85°E-95°E) and South region (SR; 8°N-15°N; 75°E-80°E). Using data from 1996 to 2013, the monthly climatology of the LFR for ER, SR, and NR is computed in order to examine the monthly fluctuations of flash rates over the areas of extreme LFR. The values of the monthly climatology of LFR over ER and SR reveal that they peak twice a year, in April-May, then again in September-October. The ER region is renowned for its severe thunderstorm conditions during the spring season, commonly referred to as Nor'westers. Intense convection brought on by the strong solar heating of the land mass during this time of year is coupled with warm, humid air from the Bay of Bengal increasing the CAPE (Penki and Kamra, 2013). Thunderstorm activity over coastal regions like ER and SR is enhanced during the spring and the monsoon withdrawal phase when more low pressure systems form over the Arabian Sea and Bay of Bengal This accounts for the dual peaks observed in LFR over these regions. LFR over NR exhibits a single maximum in June and July, followed by a sharp decline in August. Thunderstorm development over the area is aided by the semi-permanent heat

low that occurs in May and June. The enhanced updraft caused by the orographic features with elevated topography and high surface temperatures explains the increased LFR during summer over NR. High altitudes and a steep orographic gradient are favourable to the development of deep convective systems, which accounts for the high observed flash rates (Goswami et al., 2010; Kamra and Nair, 2015 Because of the low relative humidity in which they form, the thunderclouds over NR are dry and have little moisture content. Because of the high cloud base and low moisture content, the rainfall from these clouds evaporates before it reaches the ground (Penki and Kamra, 2013). Cool, moisture-laden winds restrict convection with a mild updraft once the monsoon arrives, lowering the LFR. The delayed arrival of monsoon winds over NR results in turbulent fluxes with LFR peaking in July.

		Heat content (Arabian Sea)	**Heat content (Bay of Bengal)**	**Moisture Advection (Arabian Sea)**	**Moisture Advection (Bay of Bengal)**
ER LFR	***b***	1.186×10^{-10}	5.199×10^{-11}	492.3	1774.4
	b-std	0.788	0.276	0.111	0.184
	t-value	18.57	5.75	2.05	3.21
	p	<0.0001	<0.0001	0.04	0.001
SR LFR	***b***	3.941×10^{-11}	2.067×10^{-11}	458.1	157.1
	b-std	0.705	0.296	0.277	0.044
	t-value	14.53	5.38	4.48	0.67
	p	<0.0001	<0.0001	<0.0001	0.5
NR LFR	***b***	6.175×10^{-11}	2.507×10^{-11}	-1551.8	-2740.6
	b-std	0.397	0.129	-0.337	-0.275
	t-value	10.63	3.05	-7.09	-5.45
	p	<0.0001	0.003	<0.0001	<0.0001

Table 1 Multiple regression analysis of heat content and moisture advection of the Arabian Sea and Bay of Bengal with ER, SR and NR LFR

The Arabian Sea to the west and the Bay of Bengal to the east of the Indian Peninsula act as major sources of heat and moisture, which are transported into the land region through convection. This

increases air-sea fluxes, which subsequently enhances the LFR over the land region. Lighting activity over the land area is influenced by lower tropospheric weather systems in the near-equatorial and tropical regions (Unnikrishnan et al., 2021). There is a high interannual variability and a substantial increasing trend detected in LFR from 1996 to 2013 over the NR and ER regions. Throughout the course of the study, there has also been a noticeable increase in the trend and interannual variability of heat content in the Arabian Sea and Bay of Bengal. The results using multiple regression analysis and correlation analysis indicate that moisture advection from the Arabian Sea has a significant impact on LFR over the SR region, while moisture advection from the Bay of Bengal has a higher impact on LFR over the ER region. The moisture advection from the seas had less of an impact on the LFR of the NR region. (Table 1).This area experiences dry weather during the thunderstorm's development, with little rainfall.

5. Summary

The study of "Trend and interannual variability of Arabian Sea heat content" provided insights into the underlying physical factors driving the observed warming of the Arabian Sea. This investigation suggests that the warming of the upper 300 meters in the Arabian Sea is linked to the frequency of positive Indian Ocean Dipole (IOD) and El Niño occurrences during the study timeframe. Meanwhile, it highlights that air-sea fluxes play a significant role in heating the surface mixed layer.

The study "Decadal Variability of Heat Content in the North Indian Ocean", shows a decadal signal of HC in the NIO from the surface to 700 m mainly contributed by the Arabian Sea. Our results reveal a strong relation between the decadal warming of the NIO and a corresponding warming in the South Indian Ocean (SIO), which in turn is influenced by the Western Pacific warming as well as the PDO, particularly during 2003-2017. The increased cross-equatorial flow shows a significant link to the increasing trend in Low-Level Jet and decreasing trends in Mascarene High. The study "Differential warming over the Indian Ocean", offers insights into the differential warming trends observed across the Indian Ocean between 2010 and 2022, focusing on the Arabian Sea and the Bay of Bengal. By contrasting the contrasting years of 2010 and 2019, characterized by opposing heat content patterns in the Arabian Sea and the Bay of Bengal, we explore deeper into this phenomenon. The findings from the study "Role of North Indian Ocean on the Lightning

Flash Rate of the Indian Land Region" underscore the significance of oceanic influences, even on mesoscale weather patterns over land. This correlation between moisture originating from the sea and turbulent heat exchange over land offers valuable insights into the intricate coupling of oceanic and atmospheric dynamics. Such analysis furnishes pertinent data for forthcoming research endeavors concerning heightened thunderstorm activity.

6. The Thesis

The thesis comprises seven chapters, outlined as follows

Chapter 1 provides an introduction and review of literature for the present study. The chapter provides a broad overview of energy imbalance in the climate system, brings out the importance of heat content and illustrates the increasing trend in heat content over the global ocean. The chapter explains the variability of heat content in the deep ocean. It describes different techniques used in the measurement of heat content and the errors encountered while choosing the climatology. The chapter also gives a brief introduction to wind, convection and LLJ over the Indian Ocean and their relation with heat content. Further the chapter states the objectives of the study.

Chapter 2 gives a brief description of all the datasets used in this study. This section describes the datasets used to analyze oceanic parameters like heat content, ocean heat advection, heat and volume transport, mixed layer dynamics, etc and the atmospheric parameters like air-sea fluxes, LLJ, heat fluxes, etc. The ORAS4 temperature and salinity are compared with in-situ Argo data to check the suitability of the ORAS4 data for the study in the Arabian Sea region. Surface zonal and meridional currents from ORAS4 data are compared with OSCAR data. Due to the sparse data points in ARGO during 2000-2004, the variations in ORAS4 data are compared with EN4 data. EN4.0.2 data provides quality-controlled ocean temperature and salinity profiles at the subsurface. It also provides objective analyses for uncertainty estimates, with a horizontal resolution of 1°×1°.

Chapter 3 elaborates on the extended warming patterns observed in the Arabian Sea, particularly regarding surface and subsurface heat content down to a depth of 300 m. Further, this chapter investigates the long-term trend and interannual variations of heat content in the Arabian Sea,

along with the prevailing influential processes. The chapter also gives a brief understanding of the heat budget and the variations in the MLD of the Arabian Sea during all seasons. The study also shows a significant correlation between the heat content in and below the ML indicating the possible heat exchange between the surface and subsurface layers during each season with a prolonged memory during fall and winter. The chapter includes the influence of DMI, ONI, zonal winds, air-sea flux, ocean advection and thermocline variations on the heat content of the Arabian Sea. To confirm the major results, we also performed an Empirical Orthogonal Function (EOF) analysis on the seasonal mean of heat content in ML for fall and winter and heat content below the ML down to 300 m for spring and monsoon, over the Arabian Sea from 2000 to 2017.

Chapter 4 explores the decadal variations of NIO heat content over a depth of 700 m and the transport of heat content from SIO. The study highlights the role of the Pacific in the rapid accumulation of heat in NIO and the cross-equatorial heat transfer from the SIO, on a decadal timescale. The chapter discusses the effect of changes in LLJ and Mascarene high on the heat content of NIO. LLJ shows a significant increase in strengthening, and Mascarene High shows a significant weakening trend. This Mascarene High weakening is owed to the increase in SST over the region triggered by the heat transport from the Pacific. The strengthening of LLJ drives a cross-equatorial meridional volume and heat transport. The cross-equatorial meridional volume and heat transports from SIO to NIO show their peak value at 300 m during the recent decades, hence causing a substantial increase in heat content over the region.

Chapter 5 provides an insight into the differential warming over the Indian Ocean during the recent decade from 2010 to 2022 for AS, BOB. Contrasting years 2010 and 2019 with opposite heat content patterns in the Arabian Sea and Bay of Bengal are chosen for further analysis in this study. The warmer conditions with deeper thermocline, high convection and more rainfall over the Bay of Bengal and cooler temperatures with shallow thermocline, low convection and rainfall over the Arabian Sea during 2010 and reverse conditions in the seas during 2019 are investigated in this chapter. A lag in the association between the peak phase of IOD during September-October-November and the maximum heat content during winter is observed in the study. Furthermore, a greater number of cyclones (Depressions + Cyclonic Storms + Severe Cyclonic Storms) were

observed in the Arabian Sea in 2019, whereas during 2010, they were more prevalent in the Bay of Bengal compared to the Arabian Sea.

Chapter 6 examines the correlation between heat content and moisture advection from the NIO with meteorological parameters across the Indian land region, shedding light on significant air-sea interactions. The study delves into the seasonal, monthly, and inter-annual fluctuations of lightning activity over the Indian land region and investigates the influence of the NIO on these variations. It also discusses the interannual variability in LFR and heat content of the Arabian Sea and Bay of Bengal. The findings indicate that rising heat content in the Arabian Sea and the Bay of Bengal leads to amplified moisture levels over these seas. This moisture is then carried to the Indian land region by winds during the spring and summer seasons, elevating the moisture levels over the land. Consequently, this surge in moisture triggers changes in turbulent heat fluxes over the landmass, amplifying the intensity of thunderstorms and, consequently, the frequency of lightning flashes. Multiple regression model is used to confirm the results obtained during the analyses.

Chapter 7 Summary and Conclusion of the present study

(Nisha PG)
Research Student

(Prof. TS Pranesha)
Research Guide

References:

Ali, M.M., Singh, N., Kumar, M.S., Zheng, Y., Bourassa, M., Kishtawal, C.M., Rao, C.V., 2018. Dominant modes of upper ocean heat content in the North Indian Ocean. Climate 6, 1–8. https://doi.org/10.3390/cli6030071

Annamalai, H., Murtugudde, R., 2004. Role of the Indian ocean in regional climate variability. Geophys. Monogr. Ser. 147, 213–246. https://doi.org/10.1029/147GM13

Balaguru, K., Taraphdar, S., Leung, L.R., Foltz, G.R., Knaff, J.A., 2014. Cyclone-cyclone interactions through the ocean pathway. Geophys. Res. Lett 41, 6855–6862. https://doi.org/https://doi.org/10.1002/2014GL061489

Balmaseda, MA, Trenberth, K.E., Källén, E., 2013. Distinctive climate signals in reanalysis of global ocean heat content. Geophys. Res. Lett. 40, 1754–1759. https://doi.org/10.1002/grl.50382

Balmaseda, Magdalena Alonso, Mogensen, K., Weaver, A.T., 2013. Evaluation of the ECMWF ocean reanalysis system ORAS4. Q. J. R. Meteorol. Soc. 139, 1132–1161. https://doi.org/10.1002/qj.2063

Dee, D., Coauthors, 2011. The ERA-Interim reanalysis: Configuration and performance of the data assimilation system. Quart. J. Roy. Meteor. Soc. 137, 553–597. https://doi.org/10.1002/qj.828.

Deepa, J.S., Gnanaseelan, C., Mohapatra, S., Chowdary, J.S., Karmakar, A., Kakatkar, R., Anant Parekh, 2018. The Tropical Indian Ocean decadal sea level response to the Pacific Decadal Oscillation forcing. Clim. Dyn. 52, 5045–5058. https://doi.org/10.1007/s00382-018-4431-9

Deepa, R., Seetaramayya, P., Nagar, S.G., Gnanaseelan, C., 2007. On the plausible reasons for the formation of onset vortex in the presence of Arabian Sea mini warm pool. Curr. Sci. 92, 794–800.

Dong, L., Zhou, T., Wu, B., 2014. Indian Ocean warming during 1958-2004 simulated by a climate system model and its mechanism. Clim. Dyn. 42, 203–217. https://doi.org/10.1007/s00382-013-1722-z

Dong, S., Gille, S.T., Sprintall, J., 2007. An assessment of the Southern Ocean mixed layer heat budget. J. Clim. 20, 4425–4442. https://doi.org/10.1175/JCLI4259.1

Du, Y., Xie, S.P., 2008. Role of atmospheric adjustments in the tropical Indian Ocean warming during the 20th century in climate models. Geophys. Res. Lett. 35, 2–6. https://doi.org/10.1029/2008GL033631

Duvel, J.P., Vialard, J., 2007. Indo-Pacific Sea surface temperature perturbations associated with intraseasonal oscillations of tropical convection. J. Clim. https://doi.org/10.1175/JCLI4144.1

Evan, A.T., Kossin, J.P., Chung, C.E., Ramanathan, V., 2011. Arabian Sea tropical cyclones intensified by emissions of black carbon and other aerosols. Nature 479, 94–97. https://doi.org/doi:10.1038/nature10552.

Findlater, J., 1969. A major low-level air current near the Indian Ocean during the northern summer. Q. J. R. Meteorol. Soc. 95, 362–380. https://doi.org/https://doi.org/10.1002/qj.49709540409

Gadgil, S., Rajeevan, M., Francis, P.A., 2007. Monsoon variability: Links to major oscillations over the equatorial Pacific and Indian oceans. Curr. Sci. 93, 182–194.

Gadgil, Sulochana, Vinayachandran, P.N., Francis, P.A., Gadgil, Siddhartha, 2004. Extremes of the Indian summer monsoon rainfall, ENSO and equatorial Indian Ocean oscillation. Geophys. Res. Lett. 31, 2–5. https://doi.org/10.1029/2004GL019733

Goswami, B.B., Mukhopadhyay, P., Mahanta, R., Goswami, B.N., 2010. Multiscale interaction with topography and extreme rainfall events in the northeast Indian region. J. Geophys. Res. Atmos. 115, 1–12. https://doi.org/10.1029/2009JD012275

Han, W., Meehl, G.A., Hu, A., Alexander, M.A., Yamagata, T., Yuan, D., Ishii, M., Pegion, P., Zheng, J., Hamlington, B.D., Quan, X.W., Leben, R.R., 2014a. Intensification of decadal and multi-decadal sea level variability in the western tropical Pacific during recent decades. Clim. Dyn. 43, 1357–1379. https://doi.org/10.1007/s00382-013-1951-1

Han, W., Vialard, J., McPhaden, M.J., Lee, T., Masumoto, Y., Feng, M., De Ruijter, W.P.M., 2014b. Indian ocean decadal variability: A review. Bull. Am. Meteorol. Soc. 95, 1679–1703. https://doi.org/10.1175/BAMS-D-13-00028.1

Hu, S., Fedorov, A. V., 2019. Indian Ocean warming can strengthen the Atlantic meridional overturning circulation. Nat. Clim. Chang. 9, 747–751. https://doi.org/10.1038/s41558-019-0566-x

Kamra, A.K., Nair, A.A., 2015. The impact of the Western Ghats on lightning activity on the western coast of India. Atmos. Res. 160, 82–90. https://doi.org/10.1016/j.atmosres.2015.03.006

Krishna, K.M., 2009. Intensifying tropical cyclones over the North Indian Ocean during summer monsoon-Global warming. Glob. Planet. Change 65, 12–16. https://doi.org/10.1016/j.gloplacha.2008.10.007

Krishnamurti, T. N., Molinari, J., and Pan, H. L. (1976). Numerical simulation of the Somali jet. *Journalof the Atmospheric Science*, 33, 2350–2362.

Lee, S.K., Park, W., Baringer, M.O., Gordon, A.L., Huber, B., Liu, Y., 2015. Pacific origin of the abrupt increase in Indian Ocean heat content during the warming hiatus. Nat. Geosci. 8, 445–449. https://doi.org/10.1038/NGEO2438

Lee, T., McPhaden, M.J., 2008. Decadal phase change in large-scale sea level and winds in the Indo-Pacific region at the end of the 20th century. Geophys. Res. Lett. 35, 1–7. https://doi.org/10.1029/2007GL032419

Levitus, S., Antonov, J.I., Boyer, T.P., Baranova, O.K., Garcia, H.E., Locarnini, R.A., Mishonov, A. V, Reagan, J.R., Seidov, D., Yarosh, E.S., Zweng, M.M., 2012. World ocean heat content and thermosteric sea level change (0-2000m), 1955-2010. Geophys. Res. Lett. https://doi.org/10.1029/2012GL051106

Levitus, S., Antonov, J.I., Boyer, T.P., Locarnini, R.A., Garcia, H.E., Mishonov, A. V., 2009. Global ocean heat content 1955-2008 in light of recently revealed instrumentation problems. Geophys. Res. Lett. 36, 1–5. https://doi.org/10.1029/2008GL037155

Lin, N., and Shullman, E. (2017). Dealing with hurricane surge flooding in a changing environment: Part I. Risk assessment considering storm climatology change, sea level rise, and coastal development. *Stochastic Environmental Research and Risk Assessment*, 31, 2379–2400.

Liu, W., Xie, S.P., Lu, J., 2016. Tracking ocean heat uptake during the surface warming hiatus. Nat. Commun. 7, 1–9. https://doi.org/10.1038/ncomms10926

Luo, J.-J., Sasaki, W., Masumoto, Y., 2012. Indian Ocean warming modulates Pacific climate change. Proc. Natl. Acad. Sci. 109, 18701–18706. https://doi.org/10.1073/pnas.1210239109

M., F., H., H.H., S.-P., X., G., M.A., A., S., Y., K., N., C., A, P., 2015. A. Decadal increase in Ningaloo Niño since the late 1990s. Geophys. Res. Lett. 42, 104–112. https://doi.org/https://doi.org/10.1002/2014gl062509

Madden, R.A., and Julian,P.R. (1994).Observations of the 40–50-Day Tropical Oscillation-A Review. *Monthly Weather Review*,122, 814–837.

Mantua, N.J., Hare, S.R., Y.Zhang, J.M.Wallace, Francis, R.C., 1997. A Pacific interdecadal climate oscillation with impacts on salmon production. Bull. Am. Meteorol. Soc. 78, 1069–1079.

Meehl, G.A., Arblaster, J., Fasullo, J., Hu, A., Trenberth, K., 2011. Model-based evidence of deep ocean heat uptake during surface temperature hiatus periods. Nat. Clim. Chang. 1, 360–364. https://doi.org/doi:10.1038/NCLIMATE1229

Murtugudde, R., Busalacchi, A.J., 1999. Interannual variability of the dynamics and thermodynamics of the tropical Indian Ocean. J. Clim. 12, 2300–2326. https://doi.org/10.1175/1520-0442(1999)012<2300:ivotda>2.0.co;2

Murtugudde, R., McCreary, J.P., Busalacchi, J.A., 2000. Oceanic processes associated with anomalous events in the Indian Ocean with relevance to 1997-1998. J. Geophys. Res. 105, 3295–3306. https://doi.org/https://doi.org/10.1029/1999JC900294

Murtugudde, R.G., Signorini, S.R., Christian, J.R., Busalacchi, A.J., McClain, C.R., Picaut, J., 1999. Ocean color variability of the tropical Indo-Pacific basin observed by SeaWiFS during 1997-1998. J. Geophys. Res. Ocean. 104, 18351–18366. https://doi.org/10.1029/1999jc900135

Murty, V.S.N., Krishna, S.M., Nagaraju, A., Somayajulu, Y.K., Ramesh Babu, V., Sengupta, D., Sindu, P.R., Ravichandran, M., Rajesh, G., 2006. On the warm pool dynamics in the southeastern Arabian Sea during April-May 2005 based on the satellite remote sensing and ARGO float data. Proc. SPIE 6406, Remote Sens. Mar. Environ. 640616. https://doi.org/10.1117/12.694254

Nagamani, P. V., Ali, M.M., Goni, G.J., Udaya Bhaskar, T.V.S., Mccreary, J.P., Weller, R.A., Rajeevan, M., Gopala Krishna, V. V., Pezzullo, J.C., 2016. Heat content of the Arabian Sea Mini Warm Pool is increasing. Atmos. Sci. Lett. 17, 39–42. https://doi.org/10.1002/asl.596

Nidheesh, A.G., Lengaigne, M., Vialard, J., Unnikrishnan, A.S., Dayan, H., 2013. Decadal and long-term sea level variability in the tropical Indo-Pacific Ocean. Clim. Dyn. 41, 381–402. https://doi.org/10.1007/s00382-012-1463-4

Nieves, V., Willis, J.K., Patzert, W.C., 2015. Recent hiatus caused by decadal shift in Indo-Pacific heating. Science (80-.). 349, 532–535. https://doi.org/10.1126/science.aaa4521

Penki, R.K., Kamra, A.K., 2013. The lightning activity associated with the dry and moist convections in the Himalayan Regions. J. Geophys. Res. Atmos. 118, 6246–6258. https://doi.org/10.1002/jgrd.50499

Prasanna Kumar, S., Narvekar, J., 2005. Seasonal variability of the mixed layer in the central Arabian Sea and its implication on nutrients and primary productivity. Deep. Res. Part II Top. Stud. Oceanogr. 52, 1848–1861. https://doi.org/10.1016/j.dsr2.2005.06.002

Prasanna Kumar, S., Prasad, T.G., 1999. Formation and spreading of Arabian Sea high-salinity water mass. J. Geophys. Res. Ocean. 104, 1455–1464. https://doi.org/10.1029/1998jc900022

Praveen, V., Valsala, V., Ajayamohan, R.S., Balasubramanian, S., 2020. Oceanic mixing over the northern arabian sea in a warming scenario: Tug of war between wind and buoyancy forces. J. Phys. Oceanogr. 50, 945–964. https://doi.org/10.1175/JPO-D-19-0173.1

Qiu, B., Kelly, K.A., 1993. Upper-Ocean Heat Balance in the Kuroshio Extension Region. J. Phys. Oceanogr. 23, 2027–2041. https://doi.org/https://doi.org/10.1175/1520-0485(1993)023<2027:UOHBIT>2.0.CO;2

Rao, V.B., Ferreir, C.C., Franchito, S.H., Ramakrishna, S.S.V.S., 2008. In a changing climate weakening tropical easterly jet induces more violent tropical storms over the north Indian Ocean. Geophys. Res. Lett. 35, L15710,1-4. https://doi.org/Doi:10.1029/2008GL034729

Roxy, M.K., Ghosh, S., Pathak, A., Athulya, R., Mujumdar, M., Murtugudde, R., Terray, P., Rajeevan, M., 2017. A threefold rise in widespread extreme rain events over central India. Nat. Commun. 8, 1–12. https://doi.org/10.1038/s41467-017-00744-9

Roxy, M.K., Ritika, K., Terray, P., Masson, S., 2014. The curious case of Indian Ocean warming. J. Clim. 27, 8501–8509. https://doi.org/10.1175/JCLI-D-14-00471.1

Saji, N.H., Goswami, B.N., Vinayachandran, P.N., Yamagata, T., 1999. A dipole mode in the tropical Indian Ocean. Nature 401, 360–363. https://doi.org/10.1038/43854

Saji, N.H., Yamagata, T., 2003. Structure of SST and surface wind variability during Indian Ocean Dipole mode events: COADS observations. J. Clim. 16, 2735–2751. https://doi.org/10.1175/1520-0442(2003)016<2735:SOSASW>2.0.CO;2

Sayantani, O., Gnanaseelan, C., Chowdary, J.S., 2014. The role of Arabian Sea in the evolution of Indian Ocean Dipole. Int. J. Climatol. 34, 1845–1859. https://doi.org/10.1002/joc.3805

Schott, F.A., Xie, S.P., McCreary, J.P., 2009. Indian ocean circulation and climate variability. Rev. Geophys. 47, 1–46. https://doi.org/10.1029/2007RG000245

Sengupta, D., and Ravichandran, M.(2001). Oscillations of Bay of Bengal sea surface temperature during the 1998 summer monsoon. *Geophysical research letters*, 28, 2033–2036.

Sprintall, J., Gordon, A.L., Koch-Larrouy, A., Lee, T., Potemra, J.T., Pujiana, K., Wijffels, S.E., 2014. The Indonesian seas and their role in the coupled ocean-climate system. Nat. Geosci. 7, 487–492. https://doi.org/10.1038/ngeo2188

Srinivasu, U., Ravichandran, M., Han, W., Sivareddy, S., Rahman, H., Li, Y., Nayak, S., 2017. Causes for the reversal of North Indian Ocean decadal sea level trend in recent two decades. Clim. Dyn. 49, 3887–3904. https://doi.org/10.1007/s00382-017-3551-y

Swapna, P., Jyoti, J., Krishnan, R., Sandeep, N., Griffies, S., 2017. Multi- decadal weakening of Indian summer monsoon circulation induces an increasing northern Indian Ocean sea level. Geophys Res Lett 44, 10–560. https://doi.org/doi.org/10.1002/2017G L0747 06

Thompson, P.R., Piecuch, C.G., Merrifield, M.A., McCreary, J.P., Firing, E., 2016. Forcing of recent decadal variability in the Equatorial and North Indian Ocean. J. Geophys. Res. Ocean. 121, 6762–6778. https://doi.org/10.1002/2016JC012132.Received

Timmermann, A., McGregor, S.., and Jin, F. F.(2010). Wind effects on past and future regional sea level trends in the southern Indo-Pacific. *Journal of Climate,* 23, 4429–4437.

Trenary, L.L., Han, W., 2008. Causes ofdecadal subsurface cooling in the tropical Indian Ocean during 1961–2000. Geophys Res Lett 35. https://doi.org/doi:10.1029/2008GL034687.

Trenberth, K.E., Cheng, L., Jacobs, P., Zhang, Y., Fasullo, J., 2018. Hurricane Harvey Links to Ocean Heat Content and Climate Change Adaptation. Earth's Futur. 6, 730–744. https://doi.org/https://doi.org/10.1029/2018EF000825

Ummenhofer, C., Sen Gupta, A., Li, Y., Taschetto, A.S., England, M.H., 2011. Multi-decadal modulation of the El Niño–Indian monsoon relationship by Indian Ocean variability. Environ. Res. Lett. 6. https://doi.org/doi:10.1088/1748-9326/6/3/034006.

Unnikrishnan, C.K., Pawar, S., Gopalakrishnan, V., 2021. Satellite-observed lightning hotspots in India and lightning variability over tropical South India. Adv. Sp. Res. https://doi.org/10.1016/j.asr.2021.04.009

Vidya, P.J., Balaji, M., Mani Murali, R., 2021. Cyclone Hudhud-eddy induced phytoplankton bloom in the northern Bay of Bengal using a coupled model. Prog. Oceanogr. 197, 102631. https://doi.org/10.1016/j.pocean.2021.102631

Vidya, P.J., Ravichandran, M., Subeesh, M.P., Chatterjee, S., Nuncio, M., 2020. Global warming hiatus contributed weakening of the Mascarene High in the Southern Indian Ocean. Sci. Rep. 10, 16–19. https://doi.org/10.1038/s41598-020-59964-7

Vinayachandran, P.N., Iizuka, S., Yamagata, T., 2002. Indian Ocean dipole mode events in an ocean general circulation model. Deep. Res. Part II Top. Stud. Oceanogr. 49, 1573–1596. https://doi.org/10.1016/S0967-0645(01)00157-6

Wang, B., Xu, S., Wu, L., 2012. Intensified Arabian Sea tropical storms. Nature 489. https://doi.org/doi:10.1038/489502c

Webster, P.J., Moore, A.M., Loschnigg, J.P., Leben, R.R., 1999. Coupled ocean-atmosphere dynamics in the Indian Ocean during 1997-98. Nature 401, 356–360. https://doi.org/10.1038/43848

Yamagata, T., Behera, S.K., Luo, J.J., Masson, S., Jury, M.R., Rao, S.A., 2004. Coupled ocean-atmosphere variability in the tropical Indian ocean. Geophys. Monogr. Ser. 147, 189–211. https://doi.org/10.1029/147GM12

Yang, L., Murtugudde, R., Zhou, L., Liang, P., 2020. A Potential Link Between the Southern Ocean Warming and the South Indian Ocean Heat Balance. J. Geophys. Res. Ocean. 125, e2020JC016132. https://doi.org/10.1029/2020JC016132

Yu, J.-Y., 2008. Understanding the El Niño–Southern Oscillation and its interactions with the Indian Ocean and monsoon, K. N. Liou. ed, Recent Progress in Atmospheric Sciences with Applications to the Asia-Pacific Region.

Yu, J.Y., Mechoso, C.R., McWilliams, J.C., Arakawa, A., 2002. Impacts of the Indian Ocean on the ENSO cycle. Geophys. Res. Lett. 29. https://doi.org/doi:10.1029/2001GL014098.

Zhang, Y., Feng, M., Du, Y., Phillips, H.E., Bindoff, N.L., McPhaden, M.J., 2018. Strengthened Indonesian Throughflow Drives Decadal Warming in the Southern Indian Ocean. Geophys. Res. Lett. 45, 6167–6175. https://doi.org/10.1029/2018GL078265

Zinke, J., Hoell, A., JM, L., Al, E., 2015. Coral record of southeast Indian Ocean marine heatwaves with intensified Western Pacific temperature gradient. Nat Commun 6, 1–9. https://doi.org/https://doi.org/10.1038/ncomms9562

List of Research publications

Nisha, P.G., Pranesha, T.S., Ravichandran, M., 2023. Role of north Indian Ocean on the lightning flash rate of the Indian land region. *Theor. Appl. Climatol.* 153, 73–86. https://doi.org/10.1007/s00704-023-04517-x

Nisha, P.G., Pranesha, T.S., Vidya, P.J., Ravichandran, M., Murtugudde, R., 2024. Trend and Interannual Variability of Heat Content over the Arabian Sea. *Journal of Marine Systems*, 242, 103935. https://doi.org/10.1016/j.jmarsys.2023.103935.